

Collaboration Pursuing Method for Multidisciplinary Design Optimization Problems

Dapeng Wang* and G. Gary Wang†

University of Manitoba, Winnipeg, Manitoba R3T 5V6, Canada

and

Greg F. Naterer‡

University of Ontario Institute of Technology, Oshawa, Ontario L1H 7K4, Canada

DOI: 10.2514/1.19472

Multidisciplinary design optimization problems are dominated by couplings among subsystems formulated from different disciplines. Effective and efficient collaboration between subsystems is always desirable when solving multidisciplinary design optimization problems. This work proposes a new sampling-based methodology, named the collaboration pursuing method, for multidisciplinary design optimization problems. In the collaboration pursuing method, a new collaboration model, reflecting both physical and mathematical characteristics of couplings in multidisciplinary design optimization problems, is formulated to guide the search of feasible design solutions. The interdisciplinary consistency among coupled state parameters in multidisciplinary design optimization problems is reflected and maintained by the collaboration model. An adaptive sampling strategy is also developed to speed up the search of local optimal solutions. The new method is implemented using MATLAB® 6.0 and successfully applied to four test problems, including an engineering design application.

Nomenclature

D	=	discrepancy of state parameters
f	=	system objective function
G	=	vector of functions associated with constraints
g	=	vector of constraints
L	=	difference between the ranking numbers of the largest and smallest feasible sample points
n	=	number of state parameters
r	=	ratio between the numbers of feasible and infeasible sample points
SP	=	speed factor of guidance functions
\mathbf{x}	=	vector of design variables, $\mathbf{x}_{cs} \cup \mathbf{x}_i _{i=1, \dots, n}$
\mathbf{x}_{cs}	=	vector of design variables shared by y_i and f , $\mathbf{x}_{csi} \cap \mathbf{x}_{csj}$, $i \neq j$, does not have to be \emptyset
\mathbf{x}_i	=	vector of disciplinary/local design variables of y_i
$\tilde{\mathbf{x}}_i$	=	vector of explicit and implicit design variables of y_i
\mathbf{Y}	=	implicit approximate function
\mathbf{Y}	=	explicit approximate function
\mathbf{Y}_i	=	function associated with y_i
\mathbf{y}	=	vector of state parameters, $\{y_1, \dots, y_n\}$
\mathbf{y}_{ci}	=	vector of state parameters output from other subsystems to subsystem i , $\{y_j\}$, $j \neq i$
σ	=	standard deviation

I. Introduction

A LARGE engineering problem often covers several complex and coupled physical disciplines/subsystems. For example, a helicopter air intake scoop design involves couplings among deicing, aerodynamic performance, and engine performance [1,2]. These disciplines usually rely on computationally intensive processes for analysis [e.g., finite element analysis (FEA) and computational fluid dynamics (CFD)]. Engineering design is driven by today's increasingly competitive global market. It is confined by all aspects of design such as performance, life-cycle cost, reliability, maintainability, vulnerability, and so forth, over the product life cycle from the concurrent engineering (CE) point of view [3]. Multidisciplinary design optimization (MDO), or multidisciplinary design synthesis, is a methodology for solving such complex and coupled engineering problems. MDO consists of a wide scope of issues including design synthesis, sensitivity analysis, approximation concepts, and optimization methods and strategies. It has been extensively reviewed in [4–10]. This paper is dedicated to a new sampling-based methodology that does not apply sensitivity analyses when solving MDO problems.

A general MDO problem is defined by

$$\begin{aligned} \min f(\mathbf{x}_{cs}, \mathbf{y}) \quad \text{subject to } y_i &= Y_i(\mathbf{x}_i, \mathbf{x}_{csi}, \mathbf{y}_{ci}) \\ i &= 1, \dots, n \quad \mathbf{g} = \mathbf{G}(\mathbf{x}, \mathbf{y}) \leq 0 \end{aligned} \quad (1)$$

In Eq. (1), \mathbf{y} is governed by

$$\begin{cases} y_1 = Y_1(\mathbf{x}_1, \mathbf{x}_{cs1}, \mathbf{y}_{c1}) \\ \dots \\ y_i = Y_i(\mathbf{x}_i, \mathbf{x}_{csi}, \mathbf{y}_{ci}) \\ \dots \\ y_n = Y_n(\mathbf{x}_n, \mathbf{x}_{csn}, \mathbf{y}_{cn}) \end{cases} \quad (2)$$

Equation (2) describes the system analysis (SA) or the multidisciplinary analysis (MDA). The solution of Eq. (2) is normally calculated by an iterative procedure (such as the Gauss–Seidel iterative method for linear equations and the steepest descent method for nonlinear equations [11]), when given a set of \mathbf{x} , the initial guess of \mathbf{y} , convergence criterion determined by a specified

Presented as Paper 2204 at the 1st AIAA Multidisciplinary Design Optimization Specialist Conference, Austin, TX, 18–21 April 2005; received 14 August 2005; revision received 15 July 2006; accepted for publication 21 September 2006. Copyright © 2007 by Dapeng Wang, G. Gary Wang, and Greg F. Naterer. Published by the American Institute of Aeronautics and Astronautics, Inc., with permission. Copies of this paper may be made for personal or internal use, on condition that the copier pay the \$10.00 per-copy fee to the Copyright Clearance Center, Inc., 222 Rosewood Drive, Danvers, MA 01923; include the code 0001-1452/07 \$10.00 in correspondence with the CCC.

*Ph.D., Department of Mechanical and Manufacturing Engineering, 75A Chancellors Circle; DapengWang@yahoo.com. Member AIAA.

†Associate Professor, Department of Mechanical and Manufacturing Engineering, 75A Chancellors Circle; gary_wang@umanitoba.ca. Member AIAA.

‡Professor and Director of Research, Graduate Studies and Development, Faculty of Engineering and Applied Science, 2000 Simcoe Street North; Greg.Naterer@uoit.ca. Member AIAA.

accuracy tolerance, and maximum number of iterations. State parameters \mathbf{y} usually represent some physical features (e.g., temperature) and they are often calculated by computationally intensive processes. The standard MDO formulation in Eq. (1) is also called the *multidisciplinary feasible* (MDF) method in the nonlinear programming community and the *all-in-one* method in the engineering community [12]. It can be solved by conventional optimization algorithms such as gradient-based methods, treating the SA/MDA as equality constraints. The main difficulty of applying the all-in-one method in practice is that the computational cost could be prohibitive, because the SA/MDA is frequently called during the optimization process. From this sense, reducing the number of calls to the SA/MDA can improve the performance on an MDO method.

From the engineering perspective, decomposition strategies have been applied to formulate and solve MDO problems. Global sensitivity equations (GSEs) are used in linear decomposition methods such as concurrent subspace optimization (CSSO) [13–17] and bilevel integrated system synthesis (BLISS) [18,19]. The linear decomposition methods linearize a coupled design system in the neighborhood of a feasible design. It can be imagined that the optimum solution will be reached along a piecewise path in the design variable space. Therefore, a local optimum solution could eventually result. Another decomposition-based MDO method is collaborative optimization (CO) [20–23], which uses slack variables to decouple subsystems. It was found that CO has difficulties preserving the standard Karush–Kuhn–Tucker condition due to its formulation structure [24,25]. Furthermore, a converged solution is not guaranteed. This work is motivated by a novel collaboration model, which is constructed based on the expression of couplings from mathematical and physical perspectives. This collaboration model has a similar role to GSEs for maintaining the interdisciplinary consistency of couplings in a sampling-based optimization process.

The proposed new methodology, named the *collaboration pursuing method* (CPM), aims to search for the global optimum solution of an MDO problem with a short turnaround time. It maintains the consistency of couplings among state parameters by a collaboration model implemented with radial-basis functions (RBFs). The mode-pursuing sampling (MPS) method is applied as a global optimizer module in the CPM [26,27]. Sec. II introduces the proposed collaboration model. Secs. III and IV briefly review the radial-basis function, and the MPS method, respectively. The algorithm of the CPM will be elaborated in Sec. V, and results of test cases are shown in Sec. VI.

II. Collaboration Model

MDO problems are dominated by couplings among state parameters. Effective and efficient collaboration between subsystems (i.e., interdisciplinary consistency) is always desirable when solving MDO problems. Collaboration among subsystems in linear decomposition methods is maintained by GSEs. In CO, coupled subsystems are relaxed by issuing some slack variables from the system level to disciplinary analyses. Then the interdisciplinary consistency is pursued in the system level by extra equality constraints, which are the match between the targets issued from the system level and their corresponding values returned from subsystems.

In a sampling process, it is not certain if any set of design variables \mathbf{x} can produce feasible values of its state parameters, governed by Eq. (2). This section introduces a collaboration model to help screen out, from a sample pool, infeasible sample points and select feasible sample points subject to the SA/MDA. A feasible sample subject to the SA/MDA means that the sample satisfies the simultaneous equations defined in Eq. (2). A feasible sample covers “feasibility” associated with both the physical constraints of subsystems, as well as the interdisciplinary consistency. Selected samples, by which the optimization process is further improved, have a high probability of maintaining the consistency of coupled disciplines. Therefore, the collaboration model can be viewed as a filter for a sampling process. Specifically, this collaboration model can be elaborated by using a general two-state-parameter SA/MDA problem, defined by

$$y_1 = Y_1(\mathbf{x}_1, \mathbf{x}_{cs1}, y_2) \quad y_2 = Y_2(\mathbf{x}_2, \mathbf{x}_{cs2}, y_1) \quad (3)$$

In Eq. (3), y_1 is an explicit function reflecting the physical relation between y_1 and its variables (i.e., \mathbf{x}_{cs1} , \mathbf{x}_1 , and y_2). Meanwhile, y_1 is an implicit function of \mathbf{x} , which is the union of \mathbf{x}_1 , \mathbf{x}_2 , \mathbf{x}_{cs1} , and \mathbf{x}_{cs2} . The situation is similar for y_2 . Intrinsically, all state parameters \mathbf{y} are only implicitly affected by their associated design variables. The implicit function of state parameters uncovers mathematical dependencies between state parameters \mathbf{y} and design variables \mathbf{x}_{cs1} , \mathbf{x}_1 , \mathbf{x}_{cs2} , and \mathbf{x}_2 .

Recall Eq. (2), in which the proposed collaboration model is constructed based on two dependent approximations of coupled state parameters. One is the approximation of the implicit function and the other is for the explicit function. This work employs an RBF to model the implicit and explicit approximations, as follows:

$$\bar{y}_i = \bar{Y}_i(\tilde{\mathbf{x}}_i), \quad i = 1, \dots, n \quad (4)$$

$$\bar{\bar{y}}_i = \bar{\bar{Y}}_i(\mathbf{x}_i, \mathbf{x}_{csi}, \bar{y}_{ci}), \quad i = 1, \dots, n \quad (5)$$

where $\tilde{\mathbf{x}}_i$ includes all associated design variables of the state parameter y_i , evaluated by the approximate implicit function. In MDO problems in which all state parameters are coupled with each other (in other words, values of \mathbf{y} are evaluated simultaneously with a SA/MDA), $\tilde{\mathbf{x}}_i$ is the same as \mathbf{x} defined in Eq. (1). For example, $\tilde{\mathbf{x}}_i$ is the union of \mathbf{x}_1 , \mathbf{x}_2 , \mathbf{x}_{cs1} , and \mathbf{x}_{cs2} in Eq. (3). In other situations in which at least one state parameter is not coupled with any of other state parameters [i.e., \mathbf{y}_{ci} is empty in the y_i function in Eq. (1)], and some or all of its design variables do not exist in other coupled state parameters' function, $\tilde{\mathbf{x}}_i$ is a subset of \mathbf{x} . In general, the dependency analysis of state parameters is necessary to determine which state parameter should be in Eq. (2) and which design variable should be considered in the collaboration model. The value of y_i calculated by the approximate implicit function, Eq. (4), is represented by \bar{y}_i , and sequentially, the approximate value of y_i marked as $\bar{\bar{y}}_i$ can be explicitly evaluated by Eq. (5), given \mathbf{x}_i , \mathbf{x}_{csi} , and \bar{y}_{ci} . For a set of given design variables \mathbf{x} , the interdisciplinary consistency/discrepancy of state parameters D can be determined by

$$D = \sum_{i=1}^n |\bar{y}_i - \bar{\bar{y}}_i| \quad (6)$$

If the value of D is small, then this set of design variables \mathbf{x} is possibly feasible subject to the SA/MDA.

The collaboration model defined in Eqs. (4–6) gives a distribution of the interdisciplinary discrepancy/consistency subject to the SA/MDA to a group of samples. It means that samples with a smaller value of D are more likely feasible subject to the SA/MDA than those with a larger value of D . The effectiveness of the collaboration model is shown by applying the collaboration model to a problem, which is the SA/MDA process of test case 1 (in Sec. VI), defined by

$$y_1 = x_1 + x_2 - 2 + (y_2/1.5)^4 \quad y_2 = x_3 + x_4 - 2 + (y_1/1.8)^4$$

subject to $1 \leq x_1, x_2, x_3, x_4 \leq 1.9$ (7)

In total, 100 random samples generated in the design variable space (x_1, x_2, x_3, x_4) are applied for studying the effectiveness of the proposed collaboration model. Five experimental points, listed in Table 1, are randomly generated and used for the RBF approximations defined in Eqs. (4) and (5). After applying the collaboration model for calculating the interdisciplinary discrepancy/consistency value D of the 100 random samples, the distribution of D over the 100 samples is depicted in an ascending order in terms of the value of D in Fig. 1. The real feasibility of the 100 samples subject to the SA/MDA in Fig. 1 is determined based on evaluations of \mathbf{y} of the 100 samples by calling the SA/MDA process. Samples marked with dots are feasible, and samples plotted with plus signs are infeasible. As expected, the samples with a small value of D

Table 1 Experimental points for the RBF approximation

Experiments	x_1	x_2	x_3	x_4	y_1	y_2
1	1.306581	1.398711	1.007338	1.048180	0.705300	0.079091
2	1.430430	1.504102	1.106891	1.172904	0.937613	0.353416
3	1.472354	1.571369	1.160585	1.242747	1.058492	0.522912
4	1.047014	1.668556	1.249554	1.318132	0.740550	0.596337
5	1.108217	1.734028	1.302309	1.383587	0.904644	0.749696

in Fig. 1 are more possibly feasible subject to the SA/MDA than other samples with a large value of D . The effectiveness of the collaboration model was also demonstrated in [27] by implementing the preceding study with 500 and 1000 random samples, respectively.

Because the collaboration model is built on the response surface model (i.e., radial-basis functions), an intensive study of the collaboration model was conducted in [28]. In particular, the relation between the effectiveness of the collaboration model and the accuracy of the RBF models can be shown by testing a SA/MDA problem defined in Eq. (8):

$$y_1 = e^{x_1} + 0.01y_2^2 \quad y_2 = e^{x_2} + 0.01y_1^2 \quad (8)$$

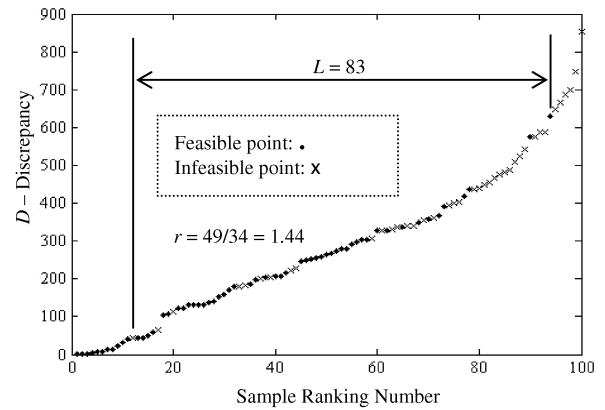
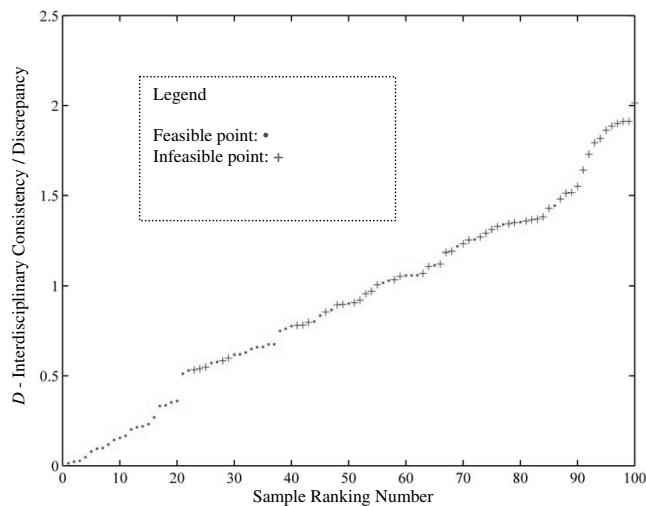
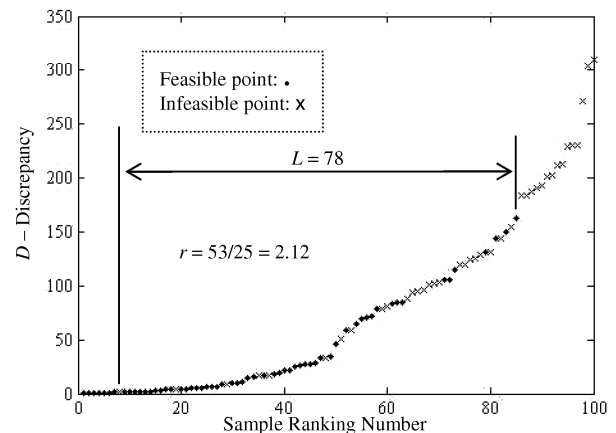
where $3.5 \leq x_1 \leq 4.5$ and $0 \leq x_2 \leq 1$. A fixed set of random samples (100) are used to demonstrate the improvement of the collaboration model with more accurate RBF models. From the point of view of approximation modeling, the accuracy of the RBF models should be improved with more experimental points. In this paper, two–six experimental points are sequentially chosen from Table 2, respectively, for setting up the RBF models needed by the collaboration model. Each collaboration model yields a distribution of the 100 samples' discrepancy of coupled state parameters in an ascending order in Figs. 2–4. Also, the feasibility of the 100 samples is checked by calling the SA/MDA and it is represented with dots (feasible) or plus signs (infeasible). As aforementioned, the purpose of the collaboration model is to separate feasible and infeasible sample points subject to the SA/MDA, based on the samples' discrepancy distribution. The length of an overlapped segment L (equal to the largest feasible sample's ranking number, the smallest infeasible sample's ranking number) with feasible and infeasible samples in Figs. 2–4 and the ratio of the feasible sample number to the infeasible sample number r in the overlapped segment indicate the effectiveness the collaboration model. In general, the shorter overlapped segment and the larger ratio (or smaller ratio for other cases) imply a more effective collaboration model. As shown in Figs. 2–4, r is increased from 1.44 based on a low-accuracy RBF model to 5.125, and the length of the overlapped segment of the discrepancy distribution curve is reduced from 83 to 49. From this

Table 2 Experimental points for the study of the collaboration model

Experiments	x_1	x_2	y_1	y_2
1	3.503310	0.347277	35.114669	13.745608
2	3.804635	0.199845	54.413245	30.829225
3	3.687938	0.792564	45.010857	22.468824
4	3.750904	0.903145	50.232818	27.700710
5	3.618321	0.841266	40.904291	19.050912
6	3.384046	0.334936	30.655226	10.795279

demonstration, the effectiveness of the collaboration model can be improved by accurate RBF models.

The collaboration model is constructed by two mutually dependent approximation functions, which reflect both physical characteristics and mathematical dependency of the SA/MDA. Samples are distinguished by a feasibility distribution subject to the SA/MDA in terms of their interdisciplinary discrepancy/consistency values determined by the collaboration model. The collaboration model serves a key role in the CPM and could be a general method for

**Fig. 2** Distribution of D of 100 random samples with two experimental points.**Fig. 1** Distribution of D , interdisciplinary consistency/discrepancy of 100 random samples.**Fig. 3** Distribution of D of 100 random samples with four experimental points.

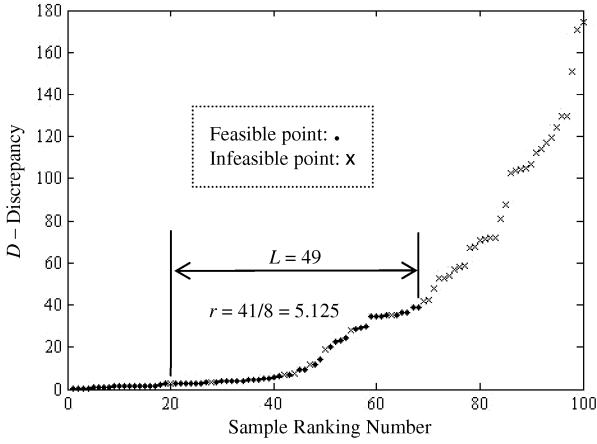


Fig. 4 Distribution of D of 100 random samples with six experimental points.

other sampling-based MDO methods. More details about the collaboration model are documented in [27,28].

III. Review of the Radial-Basis Function

The RBF can implement an $R^m \rightarrow R^1$ nonlinear mapping from the design variable space (of a state parameter y_i) \mathbf{x} to y_i , where m is the dimensionality of design variables \mathbf{x} [29]. The nonlinear mapping becomes more accurate with more experimental points. In general, given a set of E different design variables $\{\mathbf{x}^{(e)} \in R^m, e = 1, 2, \dots, E\}$ and a corresponding set of E real numbers $\{y_i^e \in R^1 | e = 1, \dots, E\}$, the RBF can be expressed in the following form.

$$\tilde{y}_i(\mathbf{x}) = p(\mathbf{x}) + \sum_{e=1}^E \alpha_i \varphi(\|\mathbf{x} - \mathbf{x}^{(e)}\|) \quad (9)$$

where p is a linear polynomial; $\tilde{y}_i(\mathbf{x}^{(e)}) = y_i^e$, $\{\varphi(\|\mathbf{x} - \mathbf{x}^{(e)}\|), e = 1, 2, \dots, E\}$ is a set of E functions, known as radial-basis functions; $\|\bullet\|$ denotes a norm, which is usually Euclidean; and α_i are unknown coefficients (weights) calculated by a set of simultaneous linear equations. The input data points $\mathbf{x}^{(e)} \in R^m, e = 1, 2, \dots, E$ are used as centers of the radial-basis functions. There is a large class of radial-basis functions including the multiquadrics, inverse multiquadrics, Gaussian functions, thin-plate spline, linear radial-basis function, etc. For simplicity, we choose the linear radial-basis function in this work, as follows:

$$\tilde{y}_i(\mathbf{x}) = \sum_{e=1}^E \alpha_i \|\mathbf{x} - \mathbf{x}^{(e)}\| \quad (10)$$

According to Micchelli's theorem [29,30], as long as $\{\mathbf{x}^{(e)}\}_{e=1}^E$ is a set of distinct points, Eq. (10) is not singular in the solution for α_i . The reason to choose the RBF is because the RBF approximation passes through all experimental points and gives a good accuracy around the experimental points. Also, it is easy to implement. The linear radial-basis function is applied to Eqs. (4) and (5) for implementing the collaboration model. It is to be noted that from the algorithm of the CPM, the RBF model is only used as a guide for sampling rather than as a surrogate of the original function based on which optimization is performed. Also, though the RBF is chosen as the approximation method in this work, neither the collaboration model nor the CPM dictates the exclusive use of the RBF.

IV. Review of Mode-Pursuing Sampling Method

The MPS method is used as a global optimizer in the CPM and it is thus briefly introduced in this section. The MPS was developed as a method to search for the global optimum of a black-box function. It is a discriminative sampling method that generates more sample points around the current minimum than other areas, while statistically

covering the entire search space [31]. The main procedure of the MPS can be elaborated when solving Eq. (11) (the general formulation of an optimization problem), as follows:

$$\min f(\mathbf{x}) \quad \text{subject to } \mathbf{g}(\mathbf{x}) \leq 0 \quad (11)$$

1) Generate ki initial experimental points through a random sampling process in the design variable space: $\mathbf{x}^{(1)}, \mathbf{x}^{(2)}, \dots, \mathbf{x}^{(ki)}$, and evaluate their corresponding objective function values of f : $f(\mathbf{x}^{(1)}), f(\mathbf{x}^{(2)}), \dots, f(\mathbf{x}^{(ki)})$. The objective function f in Eq. (11) is approximated with a radial-basis function in Eq. (12), based on all currently available function values, that is, $f(\mathbf{x}^{(1)}), f(\mathbf{x}^{(2)}), \dots, f(\mathbf{x}^{(ki)})$.

$$\hat{f}(\mathbf{x}) = \sum_{e=1}^{ki} \alpha_i \|\mathbf{x} - \mathbf{x}^{(e)}\| \quad (12)$$

such that $\hat{f}(\mathbf{x}^{(e)}) = f(\mathbf{x}^{(e)})$, $e = 1, \dots, ki$.

2) Randomly create a large number of sample points p (e.g., $p = 10^4$) in the design variable space $[\mathbf{x}_{Lb}, \mathbf{x}_{Ub}]$. All samples' approximated objective function values, $\hat{f}(\mathbf{x}_q)$ ($q = 1, \dots, p$), are evaluated by Eq. (12). A distribution GF , as shown in Fig. 5a, is defined by ranking p samples in an ascending order in terms of the value of $\hat{f}(\mathbf{x}_q)$.

3) Define a guidance function $\overline{GF}(\mathbf{x}_q)$ based on the GF distribution generated in step 2, as follows:

$$\overline{GF}(\mathbf{x}_q) = c_0 - \hat{f}(\mathbf{x}_q), \quad q = 1, \dots, p \quad (13)$$

where c_0 is a constant such that $c_0 \geq \hat{f}(\mathbf{x}_q)$, $q = 1, \dots, p$, as shown in Fig. 5b.

4) Cumulatively sum up $\overline{GF}(\mathbf{x}_q)$ over p samples to build up a new function $CG(\mathbf{x})$ by

$$CG(\mathbf{x}_q) = \frac{\sum_{j=1}^q \overline{GF}(\mathbf{x}_j)}{\sum_{i=1}^p \overline{GF}(\mathbf{x}_i)}, \quad q = 1, \dots, p \quad (14)$$

$CG(\mathbf{x})$ is plotted in Fig. 5c. This new function is used as a guide for sampling. It reflects a certain "bias" to a random selection from the set of \hat{f} ($q = 1, \dots, p$) due to its upper convex shape. In other words,

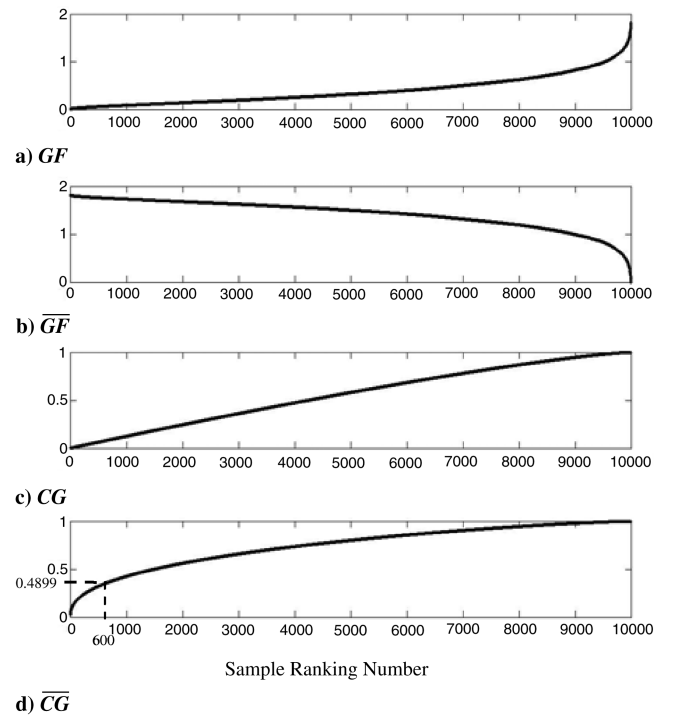


Fig. 5 Construction of the sampling guidance function.

the probability of being selected for each sample in the space of \hat{f} ($q = 1, \dots, p$) is not equal. Instead, samples with a small value of $CG(\mathbf{x})$ have a higher probability to be selected than other design samples with a large value of $CG(\mathbf{x})$.

5) Furthermore, applying a speed factor SP ,[§] the intensity of preference of $CG(\mathbf{x})$ to samples for which the value of \hat{f} is small can be increased by

$$\overline{CG}(\mathbf{x}_q) = [CG(\mathbf{x}_q)]^{SP}, \quad 0 < SP \leq 1, \quad q = 1, \dots, p \quad (15)$$

As a result, a certain number of samples will be selected randomly by a one-to-one mapping between a series of random values generated within $[0, 1]$ and samples' indices based on the distribution of $\overline{CG}(\mathbf{x})$, as shown in Fig. 5d. For example, a random value is given as 0.4899. Its corresponding sample ranking number is 600 in Fig. 5d. Then the sample with the ranking number of 600 in $CG(\mathbf{x})$ is chosen as one of the new experiments. In this way, more samples with low-ranking number values are selected than those with high-ranking number values for the next sampling iteration. The total number of chosen samples is usually between three and five.[¶]

6) Use all experiments, including the initial experiments, to form Eq. (12). Then repeat steps 2–6 until a certain convergence criterion is satisfied.

In [31], constraints \mathbf{g} are considered to be inexpensive functions of design variables \mathbf{x} . Therefore, samples violating \mathbf{g} are discarded in the random sampling process in step 2 before approximating f . This situation, however, rarely happens in MDO problems because \mathbf{g} involves state parameters, which are usually evaluated by computationally expensive processes. In each iteration, most new experiments are selected from samples in which a small value of \hat{f} exists. Meanwhile, samples are also chosen from other potential areas, even though these samples have a large value of \hat{f} . The MPS is thus, in essence, a discriminative sampling method. Compared with other optimization methods applying approximation techniques, the MPS retains the possibility to pursue the optimum solution, not only along the direction with a high gradient value, but also statistically in other potential directions. The way that MPS works is reasonable because the accuracy of approximations is uncertain and depends on many factors. It can be proved that the MPS converges to the global optimum of $f(\mathbf{x})$, as long as $f(\mathbf{x})$ is continuous in the neighborhood of the global optimum [31]. Based on the idea of building a guidance function, MPS can be customized and applied to other problems, such as multi-objective optimization [32]. In the next section, the framework of the collaboration pursuing method will be explained.

V. Collaboration Pursuing Method

The collaboration pursuing method (CPM) is a sampling-based method. The basic idea of the CPM is to select some sample candidates from a sample pool for optimization. These selected samples are preferred to be feasible subject to the SA/MDA and constraints. The collaboration model introduced in Sec. II is applied for choosing feasible samples subject to the SA/MDA. Iteratively, the CPM selects some sample candidates from a sample pool to search for the global optimum solution. The architecture of the CPM is shown in Fig. 6. The global optimum solution is achieved with the MPS method in the CPM. Because the effectiveness and efficiency of sampling-based methods are related to the number of design variables as well as the range of design variables, an adaptive sampling process is applied within the neighborhood of the current best solution \mathbf{x}^* , which is similar to a trust region [33]. Similar work has been done in [34], whereas the adaptive sampling in this work is much simpler.

The detailed process of the CPM is elaborated, incorporating Fig. 7, as follows:

[§]The value of SP is up to the designers. In general, a small SP could result in a local optimum; a large SP costs more computational efforts in searching for the global optimum.

[¶]The number of new experiments depends on the designers. The more experiments chosen, the more computational cost required.

1) In initialization steps 1 and 2, the CPM starts with several initial feasible experimental points subject to both the SA/MDA and the constraints (e.g., four), by calling the SA/MDA process. This procedure is based on a random sampling process in the design variable space. Initial experiments, or samples, will be saved in the database of experiments.

2) In each CPM iteration, several sample candidates are selected from a large sample pool for optimization. From the first CPM iteration on, two sampling processes take place in the beginning of each CPM iteration.

a) In step 3, a random sampling process employed in the original design space $[\mathbf{x}_{Lb}, \mathbf{x}_{Ub}]$ is called *global sampling*. Global sampling generates p random sample points (e.g., 10^4 , which will be processed by MPS to search for the global optimum solution).

b) In step 4, a random sampling process for generating p_3 random samples in the neighborhood of the current best solution \mathbf{x}^* is called *adaptive sampling*. The idea of the adaptive sampling is to have more samples in a small region around the current best solution. If the adaptive sampling still cannot improve the objective function value with a certain number of random samples, the size of the small region should be decreased to increase the effectiveness of the adaptive sampling. As expected, the best sample in this small region is more likely by a limited number of samples. The center of the small region will be continually updated until the optimization process reaches a local optimum, as shown in Fig. 8. The adaptive sampling searches for local optimum solutions and speeds up the optimization process. The range of design variables for adaptive sampling is determined by

$$\{\mathbf{x}^* - \Delta(\mathbf{x}_{Ub} - \mathbf{x}_{Lb}), [\mathbf{x}^* + \Delta(\mathbf{x}_{Ub} - \mathbf{x}_{Lb})]\} \quad (16)$$

where Δ is a preset ratio between 5 and 30%, depending on the number of design variables and computational capacity. The value of Δ should make sure that a limited number of samples can effectively cover the local region.

3) In the collaboration model and feasibility check, steps 5 and 6, p samples from the global sampling and p_3 samples from the adaptive sampling are separately approximated with RBF approximation based on the database of experimental points by

$$\bar{y}_{q,i} = \bar{Y}_i(\bar{\mathbf{x}}_{q,i}), \quad i = 1, \dots, n, \quad (q = 1, \dots, p \text{ or } p_3) \quad (17)$$

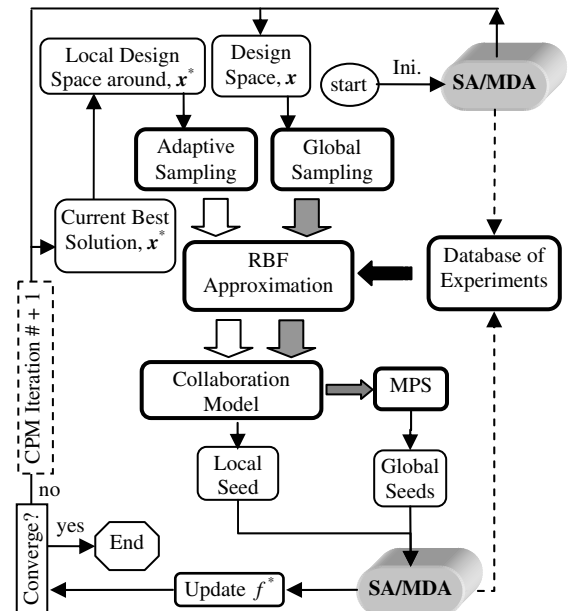


Fig. 6 Architecture of the collaboration pursuing method.

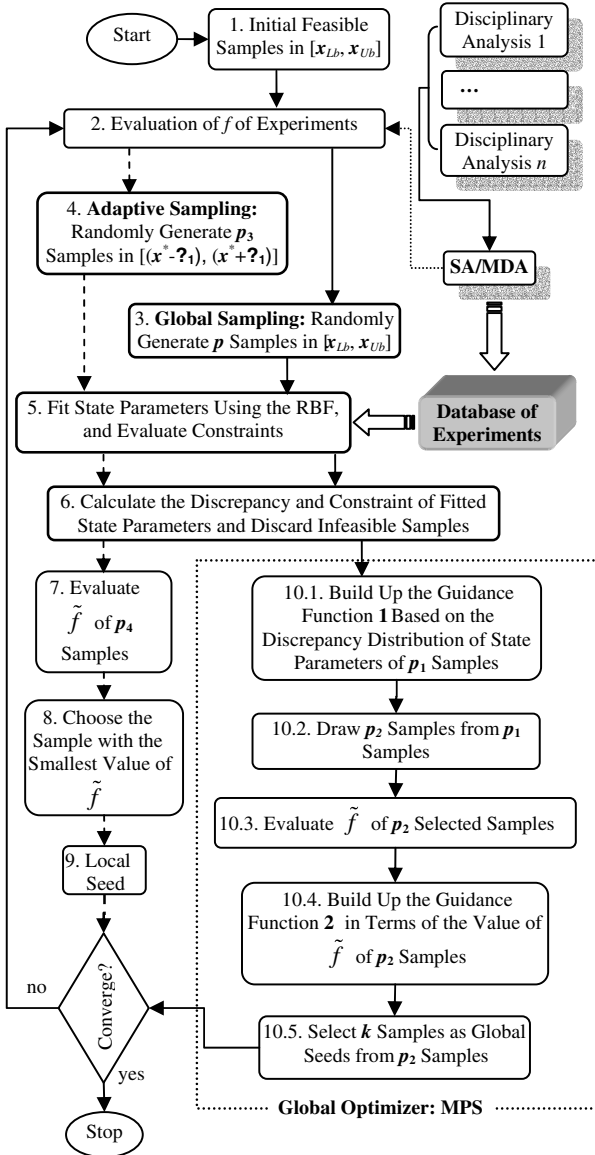


Fig. 7 Flowchart of the collaboration pursuing method.

$$\bar{\bar{y}}_{q,i} = \bar{\bar{Y}}_i(\mathbf{x}_{q,i}, \mathbf{x}_{q,csi}, \bar{\bar{y}}_{q,ci}), \quad i = 1, \dots, n \quad (18)$$

$$(q = 1, \dots, p \text{ or } p_3)$$

Samples that cannot yield matched state parameters \bar{y} by calling Eq. (2) are infeasible samples subject to the SA/MDA. The matching between coupled state parameters is maintained by the collaboration model, which filters out infeasible points subject to the SA/MDA

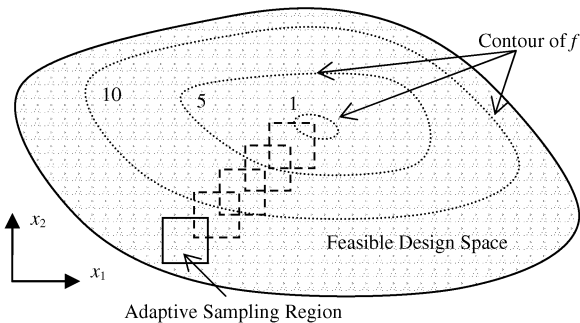


Fig. 8 Description of the adaptive sampling for a minimization problem.

based on an interdisciplinary discrepancy distribution of samples. The interdisciplinary discrepancy/consistency of each point is calculated by

$$D_q = \sum_{i=1}^n |\bar{y}_{q,i} - \bar{\bar{y}}_{q,i}|, \quad q = 1, \dots, p \text{ or } p_3 \quad (19)$$

The collaboration model shows a distribution of the interdisciplinary discrepancy/consistency subject to the SA/MDA over all samples by Eq. (19). Sequentially, the constraint check is implemented by

$$\bar{g}_q = \bar{\mathbf{G}}(\mathbf{x}_q, \bar{\mathbf{y}}_q), \quad q = 1, \dots, p \text{ or } p_3 \quad (20)$$

$$\bar{\bar{g}}_q = \bar{\bar{\mathbf{G}}}(\mathbf{x}_q, \bar{\bar{\mathbf{y}}}_q), \quad q = 1, \dots, p \text{ or } p_3 \quad (21)$$

Samples violating constraints determined by either Eq. (20) or Eq. (21) or both are discarded. This is a conservative way to make sure that selected samples are feasible subject to the constraints. The numbers of remaining samples are p_1 and p_4 , inherited from the global sampling and the adaptive sampling, respectively.

4) In steps 7–9, the approximated objective function \tilde{f} of the p_4 samples will be evaluated given design variables and $\bar{\mathbf{y}}$. For a minimization problem, a sample with the smallest value of \tilde{f} is selected as one of the new experiments, from the p_4 samples given by the adaptive sampling, and is called a local seed.

5) In step 10, global seeds (new experiments) chosen from p_1 samples are determined by the MPS method. Two guidance functions are built for this process.

a) In steps 10.1 and 10.2, p_1 samples are sorted in an ascending order in terms of the value of the interdisciplinary discrepancy/consistency given by Eq. (19). Guidance function 1 is formed by

$$GD(\mathbf{x}_q) = \sum_{i=1}^n |\bar{y}_{q,i} - \bar{\bar{y}}_{q,i}|, \quad q = 1, \dots, p_1 \quad (22)$$

Then Eq. (22) is cumulated over p_1 samples by

$$CD(\mathbf{x}_q) = \frac{\sum_{j=1}^q GD(\mathbf{x}_j)}{\sum_{i=1}^{p_1} GD(\mathbf{x}_i)}, \quad q = 1, \dots, p_1 \quad (23)$$

Finally, p_2 samples (e.g., 200) are statistically selected from a modified guidance function 1, given by

$$\overline{CD}(\mathbf{x}_q) = [CD(\mathbf{x}_q)]^{SP_1}, \quad q = 1, \dots, p_1 \quad (24)$$

The purpose of guidance function 1 is to select p_2 possibly feasible points subject to the SA/MDA and constraints.

b) In steps 10.3–10.5, the approximated objective values $\tilde{f}(\mathbf{x})$ of all p_2 samples are calculated. These p_2 samples are sorted in an ascending order in terms of $\tilde{f}(\mathbf{x})$. The guidance function 2 is built up by

$$GF(\mathbf{x}_q) = \max(\tilde{f}(\mathbf{x}_i) |_{i=1, \dots, p_2}) - \tilde{f}(\mathbf{x}_q), \quad q = 1, \dots, p_2 \quad (25)$$

Then Eq. (25) is cumulated over p_2 points by

$$CF(\mathbf{x}_q) = \frac{\sum_{j=1}^q GF(\mathbf{x}_j)}{\sum_{i=1}^{p_2} GF(\mathbf{x}_i)}, \quad q = 1, \dots, p_2 \quad (26)$$

Finally, k samples (e.g., three) are selected statistically as the new experimental points (global seeds), from a modified guidance function 2, defined by

$$\overline{CF}(\mathbf{x}_q) = [CF(\mathbf{x}_q)]^{SP_2}, \quad q = 1, \dots, p_2 \quad (27)$$

The sample with the smallest value of $\tilde{f}(\mathbf{x})$ in p_2 samples should be included in the k selected samples, because this one is promising.

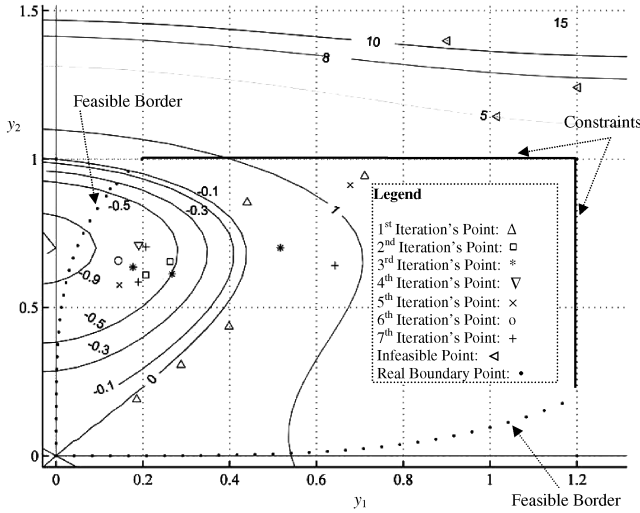


Fig. 9 Optimization process of test case 1 solved with the CPM.

6) All selected samples will be passed to the SA/MDA module to calculate the state parameters y , as well as the objective function f , in step 2. The experimental points that satisfy the SA/MDA are saved into the database of experimental points to improve the quality of the RBF approximation. The CPM can be stopped if there is no further improvement of f after a certain number of consecutive CPM iterations (e.g., six).

In summary, the collaboration model allows the CPM to extract useful information in compliance with the SA/MDA. Based on the collaboration model, the CPM uses selected samples to tune the RBF approximation model and, consequently, the RBF approximation model expands itself toward the desired solutions of MDO problems. The MPS retains the possibility to pursue the global optimum solution of MDO problems. In the next section, some test cases are solved with CPM.

VI. Test Problems and Discussion

Three numerical test cases and one engineering application are solved with CPM. The first numerical test case is formulated by the authors by placing two coupled state parameters as system variables into the well-known six-hump camelback problem. Test cases 2 and 3 are obtained from [35]. Finally, a power converter problem is solved as a benchmark MDO problem [36]. According to Figs. 6 and 7, the CPM starts with initial feasible experiments for solving all test cases. Only in test case 2 is the adaptive sampling module applied. To observe the robustness and consistency of the CPM, 10 independent runs have been carried out for each test case. The convergence tolerance of the fsolve function in MATLAB® 6.0 ([37]) for solving the SA/MDA is set to 10^{-4} in test cases 1, 2, and 4 and is set to 10^{-7} in

test case 3. For each test case, one of the 10 independent runs is randomly chosen for plotting the cumulative number of the SA/MDA evaluations over CPM iterations.

A. Test Case 1

$$\begin{aligned} \min f &= 4y_1^2 - 2.1y_1^4 + \frac{y_1^6}{3} + y_1y_2 - 4y_2^2 + 4y_2^4 \\ \text{subject to } y_1 &= x_1 + x_2 - 2 + (y_2/1.5)^4 \\ y_2 &= x_3 + x_4 - 2 + (y_1/1.8)^4 \quad y_1 \leq 1.2 \quad y_2 \leq 1.0 \\ 1 &\leq x_1, x_2, x_3, x_4 \leq 1.9 \end{aligned} \quad (28)$$

Based on an exhaustive enumeration by calling the SA/MDA, a feasible region (plotted with dots and two straight lines), subject to both the SA/MDA and constraints in the design space of the six-camel humpback problem, is shown in Fig. 9. Also, Fig. 9 shows the optimization process of the CPM by experimental points marked with different signs. The optimum solution of test case 1 should be located in the feasible region in compliance with its SA/MDA and constraints, and it should be as close as possible to $f = -0.1$, according to the contour of f in Fig. 9. Speed factors of the first and the second guidance functions are fixed as 0.51 and 0.07, respectively. At the end of each CPM iteration, four samples (global seeds) are selected. Results of test case 1 are shown in Table 3. All runs start with five feasible experiments. Runs 1 to 9 are stopped if the value of f is less than -0.9 . In particular, the optimization process of run 10 is terminated when no further improvement of f occurs after 10 consecutive CPM iterations. The convergence history of the objective function for runs 1–10 is plotted in Fig. 10. According to the objective function contour of the six-camel humpback problem in Fig. 9, the optimum is reached successfully.

B. Test Case 2

$$\begin{aligned} \min f &= y_1 + (x_2 - 2)^2 + x_3 - 2 + e^{-y_2} \\ \text{subject to } y_1 &= x_1^2 + x_2 + x_3 - 4 - 0.2y_2 \\ y_2 &= x_1 + x_3 - 2 + \sqrt{y_1} \quad 0 \leq x_1 \leq 7 \quad \text{and} \quad 2 \leq x_2, x_3 \leq 7 \end{aligned} \quad (29)$$

Speed factors of the first and the second guidance functions are fixed as 1 and 0.41, respectively. At the end of each CPM iteration, three samples (one local seed and two global seeds) are selected. Results are listed in Table 4. Runs 1–3 are stopped if the value of f is less than 8.08; runs 4–6 are stopped if the value of f is less than 8.04; and runs 7–9 are terminated after six consecutive CPM iterations with no further improvement of the value of f . All runs start with five random feasible experiments. The adaptive sampling module is applied in

Table 3 Results of test case 1

No. of run	No. of SA/MDA		Optimum value of f	Optimum value of x				Optimum value of y		
	Feasible	Infeasible		x_1	x_2	x_3	x_4	y_1	y_2	
		Initial								After init
1	55	2	0	$-9.070575e^{-1}$	1.001897	1.035303	1.526232	1.184495	0.087604	0.710732
2	28	4	0	$-9.111311e^{-1}$	1.002131	1.012684	1.355314	1.264257	0.043922	0.619571
3	20	3	0	$-9.093511e^{-1}$	1.008852	1.008468	1.078122	1.542187	0.046566	0.620309
4	36	1	0	$-9.343211e^{-1}$	1.011585	1.009576	1.594216	1.099452	0.066896	0.693671
5	57	9	0	$-9.154225e^{-1}$	1.000354	1.036599	1.312874	1.370380	0.080004	0.683258
6	26	6	0	$-9.014565e^{-1}$	1.001388	1.042767	1.296005	1.359486	0.080624	0.655495
7	35	12	0	$-9.322473e^{-1}$	1.016560	1.005368	1.489481	1.209155	0.068987	0.698638
8	58	4	0	$-9.409803e^{-1}$	1.000501	1.004792	1.451814	1.194624	0.039787	0.646438
9	29	2	0	$-9.198739e^{-1}$	1.012159	1.021370	1.506066	1.177620	0.076689	0.683689
Ave				$-9.19e^{-1}$						
σ				$1.37e^{-2}$						
10	79	6	0	$-9.477366e^{-1}$	1.002180	1.005740	1.479164	1.223990	0.056208	0.703155

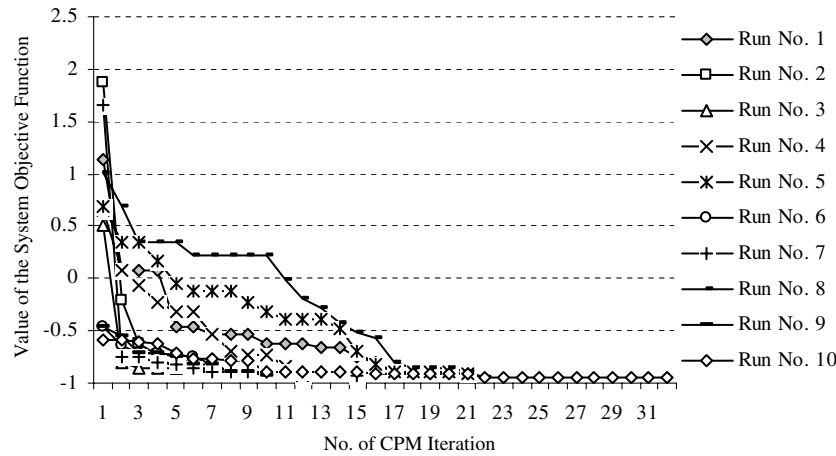


Fig. 10 Intermediate best objective function values over 32 CPM iterations of runs 1–10 in test case 1.

runs 1–9 by setting $\Delta_1 = 5\%$. It is observed that the adaptive sampling is especially efficient when the system objective function f is sensitive to the variation of its design variables. Comparisons are given between runs 1–9 and run 10, which does not apply adaptive sampling and it is stopped if the value of f is less than 8.08. Apparently, run 10 has the worst optimum value, with the highest number of calls to the SA/MDA. The convergence history of f of runs 7–9 is shown in Fig. 11.

C. Test Case 3

$$\begin{aligned} \min f &= \frac{y_1^2}{x_1} + y_2^2 - x_2 \quad \text{subject to } y_1 = \frac{x_1 y_2 y_3^2}{x_2 y_4} \\ y_2 &= \sqrt{\frac{x_1 y_3}{x_2}}, \quad y_3 = \frac{y_1 y_4}{2 x_1 y_2}, \quad y_4 = \frac{x_1 y_3^2}{x_2^2} \\ h_1 &= y_4 - y_3 - 2 = 0 \quad g_1 = y_2^2 + 1 - x_1 \geq 0 \\ 0 < x_i &\leq 1, \quad i = 1, 2 \end{aligned} \quad (30)$$

Speed factors of the first and the second guidance functions are set to 0.51 and 0.81, respectively. Upper bounds of the design variables are assigned by the authors. At the end of each CPM iteration, five samples (global seeds) are selected. The SA/MDA solver within the CPM is applied to evaluate the optimal solution given by [35] for verifying its accuracy. For the given design variable set, the optimal objective function value is the same as reported in [35], which is

2.984, as shown in Table 5 (the optimum values of y are not available in [35]). All runs are terminated after six consecutive CPM iterations without further improvement of f . All of the 10 runs start with three random feasible experiments. Results by running the CPM are shown in Table 6. The optimal function values obtained are in the neighborhood of 1.0, which is better than 2.984, given by the CSSO in [35]. It is very difficult to maintain the feasibility of samples subject to the SA/MDA in this case, because the SA/MDA is overconstrained by an equality constraint. The trend of the objective function of runs 1–10 is plotted in Fig. 12. The difficulty of achieving feasible samples, raised by the equality constraint, results in a large computational effort for initialization and an early stop of the optimization process according to the optimization convergence criterion.

D. Test Case 4

The power converter problem comprises a coupling between an electrical subsystem and a loss subsystem. An optimal power stage design is essential to the development of a quality power converter. The power stage design dominates the overall efficiency, size, and weight of the power converter. The objective of the power converter problem is to minimize the weight. The problem consists of 6 design variables and 12 state variables, of which 4 define constraints. All constant values can be referred to [36]. A schematic of the power converter problem is shown in Fig. 13, and the geometry of the transformer core is shown in Fig. 14. The formulation of the power converter problem is defined by

Table 4 Results of test case 2

No. of run	No. of SA/MDA			Optimum value of f	Optimum value of x			Optimum value of y	
	Feasible	Infeasible			x_1	x_2	x_3	y_1	y_2
		Initial	After init						
1	21	25	8	8.061338	3.016562	2.042900	2.046421	8.010318	5.893234
2	23	20	9	8.066726	3.004791	2.157272	2.011495	8.027615	5.849590
3	38	17	18	8.030440	3.020825	2.036224	2.019330	8.006974	5.869815
Ave				8.052835					
σ				0.019581					
4	33	34	10	8.021729	3.020842	2.048775	2.006903	8.009590	5.857867
5	19	5	10	8.028838	3.013692	2.093780	2.005488	8.011675	5.849671
6	68	36	14	8.034520	3.020577	2.071583	2.000979	8.025550	5.854496
Ave				8.028362					
σ				0.006409					
7	52	24	18	8.014559	3.024412	2.021236	2.007586	8.003674	5.861074
8	49	5	16	8.013545	3.022309	2.029848	2.008772	8.001031	5.859690
9	93	14	17	8.008876	3.026792	2.014285	2.000711	8.005100	5.856832
Ave				8.0123267					
σ				0.0030311					
10	161	21	7	8.075582	3.011512	2.118991	2.022045	8.036551	5.868438
Results from [35]				8.003	3.025	2.000	2.000		

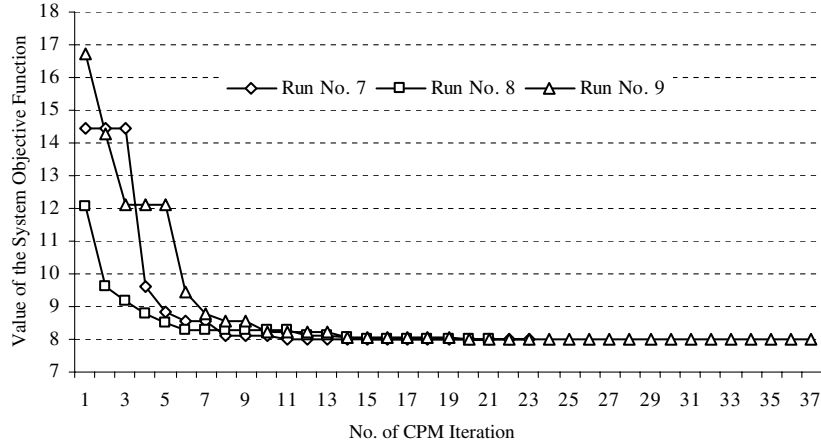


Fig. 11 Intermediate best objective function values over 37 CPM iterations of runs 7–9 in test case 2.

$$y_1 = f(x) = W_c + W_w + W_{\text{cap}} + W_{\text{hs}} \quad (31) \quad \text{the inductor value}$$

subject to the electrical design state analysis duty cycle

$$y_8 = \frac{(EO + VD)(1 - y_3)}{y_6 x_2 (FR)}$$

$$y_3 = \frac{EO}{\left(\frac{y_2 EI}{2(XN)}\right)}$$

the loss design state analysis circuit efficiency

the minimum duty cycle

$$y_2 = \frac{PO}{PS + PQ + PD + POF + P\text{XFR}}$$

$$y_4 = \frac{EO}{\left(\frac{y_2 EIMAX}{2XN}\right)}$$

the fill window constraint

the inductor resistance

$$g_1 = WA - \frac{x_3 x_2}{FW} + (-WBOB)x_6 K_2 \geq 0$$

$$y_5 = \frac{XMLT x_2 (RO)}{x_3}$$

where $WA = K_2 x_6 |x_6|$
the ripple specification

where $XMLT = 2x_1(1 + K_1)FC$

the core cross-sectional area

$$g_2 = \frac{VR - DELI(ESR)}{EO} \geq 0$$

$$y_6 = K1|x_1|x_1$$

where

the magnetic path length

$$y_7 = \frac{\pi}{2} x_1$$

$$DELI = \frac{(EO + VD)(1 - y_3)}{x_4 FR}$$

Table 5 Accuracy comparison between the CPM and the CSSO applied in [35]

Method	Optimum value of f	Optimum design of x from [35]	Optimum design of y
CPM	2.984	$x_1 = 0.998 x_2 = 0.996$	$y_1 = 1.4071$ $y_2 = 1.4128$ $y_3 = 1.9920$ $y_4 = 3.9919$
CSSO in [35]	2.984		N/A

Table 6 Results of test case 3

No. of run	No. of SA/MDA		Optimum value of f	Optimum value of x	Optimum value of y
	Feasible	Infeasible			
		Initial After init			
1	40	171 27	0.996646	$x_1 = 0.522049$ $x_2 = 0.072530$	$y_1 = 0.073801$ $y_2 = 1.028952$ $y_3 = 0.147079$ $y_4 = 2.146778$
2	35	218 20	0.938502	$x_1 = 0.447010$ $x_2 = 0.015635$	$y_1 = 0.014464$ $y_2 = 0.976560$ $y_3 = 0.033348$ $y_4 = 2.033509$
3	36	297 2	0.890401	$x_1 = 0.398669$ $x_2 = 0.005149$	$y_1 = 0.004404$ $y_2 = 0.946309$ $y_3 = 0.011567$ $y_4 = 2.011850$
4	43	180 0	1.007149	$x_1 = 0.516492$ $x_2 = 0.020540$	$y_1 = 0.020914$ $y_2 = 1.013332$ $y_3 = 0.040829$ $y_4 = 2.040768$
5	35	350 44	1.031431	$x_1 = 0.562961$ $x_2 = 0.121428$	$y_1 = 0.128897$ $y_2 = 1.059881$ $y_3 = 0.242341$ $y_4 = 2.242294$
6	18	264 0	0.966130	$x_1 = 0.477408$ $x_2 = 0.024440$	$y_1 = 0.023621$ $y_2 = 0.994687$ $y_3 = 0.050652$ $y_4 = 2.050567$
7	20	295 25	0.983973	$x_1 = 0.499534$ $x_2 = 0.036815$	$y_1 = 0.036586$ $y_2 = 1.009014$ $y_3 = 0.075030$ $y_4 = 2.074819$
8	28	69 30	0.973706	$x_1 = 0.488703$ $x_2 = 0.034050$	$y_1 = 0.033357$ $y_2 = 1.002736$ $y_3 = 0.070074$ $y_4 = 2.069790$
9	15	308 20	0.991809	$x_1 = 0.515382$ $x_2 = 0.062673$	$y_1 = 0.063319$ $y_2 = 1.023085$ $y_3 = 0.127323$ $y_4 = 2.127136$
10	16	46 45	1.129521	$x_1 = 0.628626$ $x_2 = 0.252015$	$y_1 = 0.282756$ $y_2 = 1.119979$ $y_3 = 0.502852$ $y_4 = 2.502753$
Ave			0.990927		
σ			0.062325		

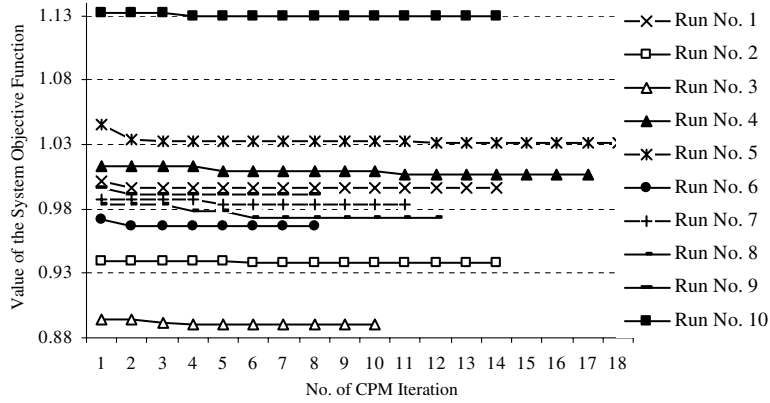


Fig. 12 Intermediate best objective function values over 12 CPM iterations of runs 1–10 in test case 3.

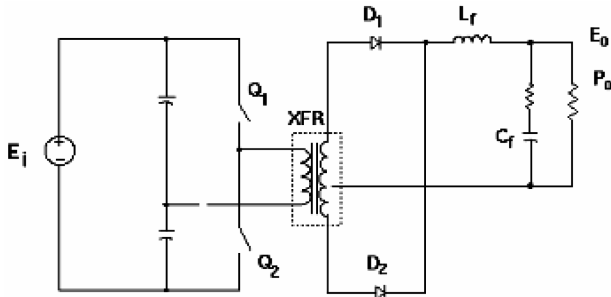


Fig. 13 A schematic of the power stage of the power converter [8,36].

the core saturation

$$g_3 = BSP - \frac{x_4(XIMAX)}{y_6 x_2} \geq 0$$

where

$$XIMAX = \frac{PO}{EO} + \frac{(EO + VD)(1 - y_4)}{2x_4 FR}$$

the minimum inductor size for continuous mode at EIMAX and POMIN

$$g_4 = x_4 - XLCRIT \geq 0$$

where

$$XLCRIT = \frac{(EO + VD)(1 - y_4)EO}{2(POMIN)FR}$$

where

$$W_c = |DI y_6 (ZP_1 + y_7)|$$

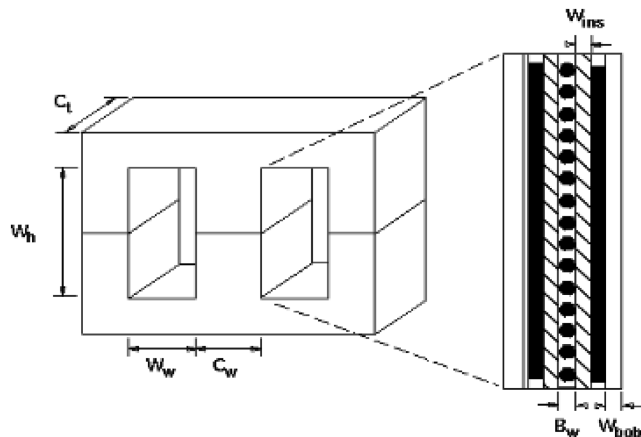


Fig. 14 The geometry of the transformer core [8,36].

$$\begin{aligned} ZP_1 &= 2(1 + K_2)x_6 \\ W_w &= |(XMLT)(DC)x_3 x_2| \\ XMLT &= 2x_1(1 + K_1)FC \\ W_{cap} &= |(DK_5)x_5| \\ W_{hs} &= |(PO/KH)[(1/y_2) - 1]| \end{aligned}$$

The power converter problem has six design variables, as shown in Table 7. Relatively large upper bounds of all design variables and the lower bound of x_4 are assigned by the authors, by referring to the optimum solution and the lower bounds of design variables from [36]. The problem is mainly dominated by the couplings among y_2 , y_3 , and y_8 , and the explicit dependency matrix is shown Table 8. Speed factors of the first and the second guidance functions are fixed as 1 and 0.00011, respectively. At the end of each CPM iteration, two samples (global seeds) are selected. Similar to test case 3, the SA/MDA solver within the CPM is applied to evaluate the optimum solution in [36] for verifying its accuracy. As shown in Table 9, the CPM has the same accuracy as the CSSO in [36]. After the verification, 10 independent optimization runs are carried out with the CPM and terminated when there is no further improvement of f after six consecutive CPM iterations, as shown in Table 10. All runs start with four random feasible experiments. The convergence of f of runs 1–10 is plotted in Fig. 15. For run 4 (with the highest number of calls to the SA/MDA in Table 10), the cumulative number of the SA/MDA at each CMP iteration step is shown in Fig. 16.

According to [36], the optimum solution ($f = 1.48$) is given by CSSO with 54 “design point system iterations,” which refers to a call of the SA/MDA. The CPM is more efficient than the CSSO for solving the power converter problem, based on the results in Tables 9 and 10.

E. Discussion

For the implementation of MPS, if the guidance function 1 [Eq. (24)] is sped up intensively by applying a small value of SP_1 (e. g., $SP_1 = 0.01$), new samples given from the current CPM iteration to the next one are most likely feasible. The speed factor value influences the efficiency of the MPS. An aggressive speed factor could lead to a local optimum, and a large speed factor value could slow down the optimization procedure. Based on the feedback from

Table 7 Design variables of the power converter problem

Variable	Name	Description	Range	
			Lower bound	Upper bound
x_1	C_w	Core center leg width	0.001	0.1
x_2	Turns	Inductor turns	1.0	10.
x_3	A_{cp}	Copper size	$7.29e^{-8}$	$1.0e^{-5}$
x_4	$L_f/PINDUC$	Inductance	$1.0e^{-6}$	$1.0e^{-5}$
x_5	C_f	Capacitance	$1.e^{-5}$	0.01
x_6	W_w	Core window width	0.001	0.01

Table 8 Dependency matrix of the power converter problem

	y_1	y_2	y_3	y_4	y_5	y_6	y_7	y_8	x_1	x_2	x_3	x_4	x_5	x_6
y_1/f		X				X	X		X	X	X		X	X
y_2			X		X	X	X	X				X	X	X
y_3		X												
y_4		X												
y_5									X	X	X			
y_6									X					
y_7									X					
y_8			X			X				X				
g_1										X	X			X
g_2			X									X		
g_3				X		X				X		X		
g_4				X								X		

Table 9 Accuracy comparison between the CPM and the CSSO applied in [36]

Method	Optimum value of f	Optimum Design of x from [36]	Optimum design of y
CPM	1.4856	$x_1 = 0.0191$ $x_2 = 4.91$ $x_3 = 0.00000677$ $x_4 = 0.00000524$ $x_5 = 0.00263$ $x_6 = 0.00759$	$y_2 = 0.8302$ $y_3 = 0.5929$ $y_4 = 0.4535$ $y_5 = 0.0018$ $y_6 = 0.0003648$ $y_7 = 0.0300$ $y_8 = 0.0128$
CSSO used in [36]	1.48		$y_2 = 0.830$ $y_3 = 0.593$ $y_4 = 0.453$ $y_5 = 0.00182$ $y_6 = 0.000367$ $y_7 = 0.0301$ $y_8 = 0.0128$

Table 10 Results of test case 4

No. of run	No. of SA/MDA		Optimum value of f	Optimum value of x	Optimum value of y	
	Feasible	Infeasible				
		Initial				After init
1	35	1	3	1.40026	$x_1 = 0.011965$ $x_2 = 5.137405$ $x_3 = 0.000008$ $x_4 = 0.000002$ $x_5 = 0.008793$ $x_6 = 0.008656$ $y_2 = 0.841751$ $y_3 = 0.584688$ $y_4 = 0.032096$ $y_5 = 0.447247$ $y_6 = 0.001006$ $y_7 = 0.000143$ $y_8 = 0.018794$	
2	30	3	1	1.46960	$x_1 = 0.018990$ $x_2 = 3.261643$ $x_3 = 0.000007$ $x_4 = 0.000002$ $x_5 = 0.006239$ $x_6 = 0.007036$ $y_2 = 0.840183$ $y_3 = 0.585882$ $y_4 = 0.019873$ $y_5 = 0.448082$ $y_6 = 0.001126$ $y_7 = 0.000361$ $y_8 = 0.029829$	
3	20	0	7	1.46435	$x_1 = 0.015288$ $x_2 = 4.819028$ $x_3 = 0.000007$ $x_4 = 0.000003$ $x_5 = 0.007675$ $x_6 = 0.007685$ $y_2 = 0.836584$ $y_3 = 0.588444$ $y_4 = 0.020638$ $y_5 = 0.450009$ $y_6 = 0.001384$ $y_7 = 0.000234$ $y_8 = 0.024015$	
4	33	6	2	1.48278	$x_1 = 0.019377$ $x_2 = 2.581968$ $x_3 = 0.000009$ $x_4 = 0.000002$ $x_5 = 0.007388$ $x_6 = 0.008073$ $y_2 = 0.845515$ $y_3 = 0.582134$ $y_4 = 0.024302$ $y_5 = 0.445256$ $y_6 = 0.000766$ $y_7 = 0.000375$ $y_8 = 0.030437$	
5	22	31	0	1.44344	$x_1 = 0.017046$ $x_2 = 3.373527$ $x_3 = 0.000008$ $x_4 = 0.000003$ $x_5 = 0.007254$ $x_6 = 0.008487$ $y_2 = 0.843580$ $y_3 = 0.583488$ $y_4 = 0.023968$ $y_5 = 0.446277$ $y_6 = 0.000903$ $y_7 = 0.000291$ $y_8 = 0.026776$	
6	25	0	4	1.49415	$x_1 = 0.020723$ $x_2 = 3.178963$ $x_3 = 0.000006$ $x_4 = 0.000004$ $x_5 = 0.004352$ $x_6 = 0.005940$ $y_2 = 0.833817$ $y_3 = 0.590396$ $y_4 = 0.016946$ $y_5 = 0.451502$ $y_6 = 0.001568$ $y_7 = 0.000429$ $y_8 = 0.032552$	
7	29	2	3	1.44674	$x_1 = 0.016082$ $x_2 = 5.453818$ $x_3 = 0.000007$ $x_4 = 0.000003$ $x_5 = 0.004478$ $x_6 = 0.007960$ $y_2 = 0.832009$ $y_3 = 0.591687$ $y_4 = 0.016351$ $y_5 = 0.452484$ $y_6 = 0.001694$ $y_7 = 0.000259$ $y_8 = 0.025262$	
8	26	9	3	1.39168	$x_1 = 0.012810$ $x_2 = 5.567491$ $x_3 = 0.000008$ $x_4 = 0.000002$ $x_5 = 0.006761$ $x_6 = 0.009895$ $y_2 = 0.840247$ $y_3 = 0.585794$ $y_4 = 0.025761$ $y_5 = 0.448048$ $y_6 = 0.001109$ $y_7 = 0.000164$ $y_8 = 0.020122$	
9	27	5	0	1.43167	$x_1 = 0.012973$ $x_2 = 7.524132$ $x_3 = 0.000008$ $x_4 = 0.000003$ $x_5 = 0.005366$ $x_6 = 0.009920$ $y_2 = 0.832640$ $y_3 = 0.591244$ $y_4 = 0.018234$ $y_5 = 0.452141$ $y_6 = 0.001669$ $y_7 = 0.000168$ $y_8 = 0.020378$	
10	29	1	0	1.396361	$x_1 = 0.015761$ $x_2 = 3.054849$ $x_3 = 0.000007$ $x_4 = 0.000002$ $x_5 = 0.007356$ $x_6 = 0.007650$ $y_2 = 0.843796$ $y_3 = 0.583243$ $y_4 = 0.031227$ $y_5 = 0.446163$ $y_6 = 0.000866$ $y_7 = 0.000248$ $y_8 = 0.024757$	
Ave				1.442103		
σ				0.036716		

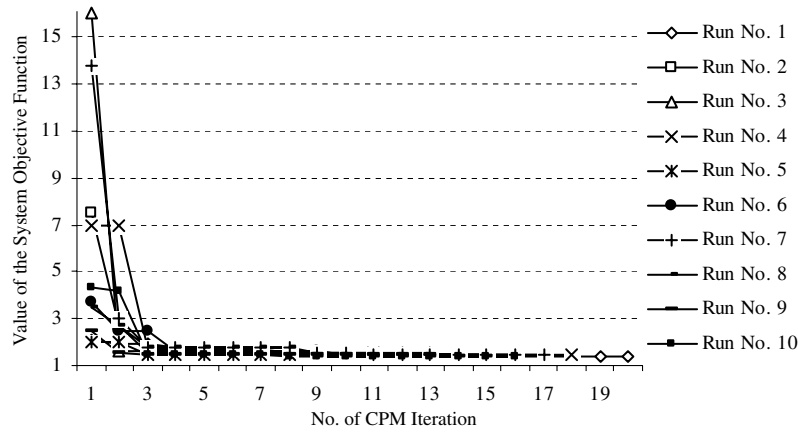


Fig. 15 Intermediate best objective function values over 18 CPM iterations of runs 1–10 in test case 4.

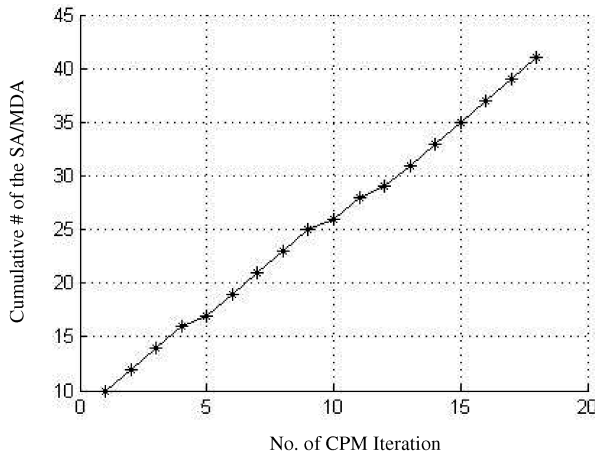


Fig. 16 Cumulative number of the SA/MDA processes over 18 CPM iterations of run 4 in test case 4.

the last CPM iteration, the speed factor could be dynamically adjusted by designers' intervention. For example, the value of the speed factor should be reduced if the value of f is not improved after several consecutive CPM iterations and the number of feasible experiments is larger than that of infeasible experiments at each CPM iteration. In this work, for fair comparison, the speed factors are fixed throughout one optimization process and fixed for a number of independent runs. The efficiency of the CPM can be potentially further improved by dynamically tuning the speed factors.

In this work, the CPM starts with feasible experimental points subject to both the SA/MDA and constraints. A common problem from all results is that the CPM spent a lot of effort on generating initial feasible experiments. As the number of state parameters and design variables increase, initialization could become a problem, and so a good initialization procedure is important. A strategy is tested to generate feasible experiments by giving a small offset to the design variables of the last feasible experimental point. Although this strategy has been shown successful, it does not guarantee that feasible experiments will be generated. A new initialization process, based on feasible experimental points subject to the SA/MDA but not necessarily to constraints, has been applied to a conceptual aircraft design problem [27,38]. More feasible experiments subject to both the SA/MDA and constraints are expected to be created after the initialization step to replace the infeasible experiments subject to the constraints in the database of experiments. This is more efficient than the current initialization process. Also, for engineering problems, experimental data and other related experience can partly alleviate such a difficulty in initialization.

The efficiency and capability of sampling-based optimization methods are dependent on the range and number of design variables. As the range and number of design variables become large, CPM

encounters difficulties caused by a limited number of samples, which cannot effectively cover the design space. The adaptive sampling showed its advantage in this regard when solving test case 2. For large-scale design problems, the key to the sampling-based optimization methods is to effectively reduce the number and range of the design variables, while maintaining the optimization progress. Because of the nature of sampling, the capability and efficiency of the CPM can be improved by applying parallel computing for generating a very large number of samples.

It is observed that the collaboration model is effective for collaborating coupled subsystems. For MDO problems, the number of coupled state parameters is usually relatively low when compared with design variables. Based on this observation, the collaboration model could still be effective in dealing with a high degree of coupling. For testing the CPM's applicability in this regard, a conceptual aircraft design problem involving 10 design variables, 12 constraints, and 3 nonlinear coupled disciplines was solved efficiently with the CPM [27].

The CPM relies on the SA/MDA rather than sensitivity analyses. From this perspective, the CPM is an all-in-one/MDF-like MDO approach, which aims to reduce the total number of calls to the SA/MDA. Its efficiency has been demonstrated through comparisons with the all-in-one/MDF in [27,38]. In general, the CPM has the same level of applicability for solving MDO problems as the all-in-one/MDF approach. The efficiency of the CPM comes from an integration of collaboration modeling, metamodeling, and sampling-based optimizers. A global search algorithm, MPS, is applied in the CPM. Because MPS is a sampling-based search algorithm and only the number of expensive function evaluation is used as the efficiency measure (the cost of evaluating metamodels is negligible compared with the cost of expensive function evaluation), MPS is thus an efficient global search scheme for expensive black-box functions. Similarly, the CPM is a sampling-based MDO approach for expensive SA/MDA processes. It selects promising samples from a sample pool, which are determined from search or optimization methods, and only a few selected sample points are evaluated expensively. Therefore, as a global search scheme, the CPM still demonstrates high efficiency from the perspective of the total number of expensive SA/MDAs.

VII. Conclusions

This paper proposed the collaboration model, which is constructed by two mutually dependent approximation functions. The collaboration model reflects both the physical and mathematical characteristics of couplings and effectively coordinates coupled subsystems for solving test cases. Based on the collaboration model, the collaboration pursuing method, as a sampling-based MDO method, is developed. The CPM uses the MPS method to search for the global optimum and uses the adaptive sampling strategy to enhance the CPM's capability to converge to local optimum solutions. Four test cases have been successfully and robustly solved

with the CPM. Future work will be focused on investigating the applicability and efficiency of the CPM for MDO problems with a large scale of design variables and a fairly large number of state parameters.

Acknowledgments

Support of this research from the Natural Sciences and Engineering Research Council (NSERC) of Canada is gratefully acknowledged. Also, the assistance of S. Shan is gratefully acknowledged.

References

- [1] Wang, D., Naterer, G. F., and Wang, G. G., "Adaptive Response Surface Method for Thermal Optimization: Application to Aircraft Engine Cooling System," AIAA/ASME 8th Joint Thermophysics and Heat Transfer Conference, St. Louis, MO, AIAA Paper 2002-3000, 2002.
- [2] Wang, D., Naterer, G. F., and Wang, G. G., "Thermofluid Optimization of a Heated Helicopter Engine Cooling Bay Surface," *Canadian Aeronautics and Space Journal le Journal Aeronautique et Spatial du Canada*, Vol. 49, June 2003, pp. 73–86.
- [3] Schrage, D., Beltracchi, T., Berke, L., Dodd, A., Niedling, L., and Sobieszcanski-Sobieski, J., *Current State of the Art on Multidisciplinary Design Optimization (MDO)*, General Publication Series, AIAA, Washington, D.C., Sept. 1991.
- [4] Sobieszcanski-Sobieski, J., and Haftka, R. T., "Multidisciplinary Aerospace Design Optimization: Survey of Recent Developments," 34th AIAA Aerospace Sciences Meeting and Exhibit, Reno, NV, AIAA Paper 96-0711, 1996, p. 32.
- [5] Balling, R. J., and Sobieszcanski-Sobieski, J., "Optimization of Coupled Systems: A Critical Overview of Approaches," *AIAA Journal*, Vol. 36, No. 1, Jan. 1996, pp. 6–17.
- [6] Kodiyalam, S., and Sobieszcanski-Sobieski, J., "Multidisciplinary Design Optimization, Some Formal Methods, Framework Requirements, and Application to Vehicle Design," *International Journal of Vehicle Design*, Vol. 25, Nos. 1–2, 2001, pp. 3–22.
- [7] Balling, R. J., and Wilkinson, C. A., "Execution of Multidisciplinary Design Optimization Approaches on Common Test Problems," *AIAA Journal*, Vol. 35, No. 1, Jan. 1997, pp. 178–186.
- [8] Kodiyalam, S., "Evaluation of Methods for Multidisciplinary Design Optimization (MDO), Phase 1," NASA CR-1998-208716, Sept. 1998.
- [9] Kodiyalam, S., "Evaluation of Methods for Multidisciplinary Design Optimization (MDO), Phase 2," NASA CR-2000-210313, Nov. 2000.
- [10] Wang, D., Naterer, G. F., and Wang, G. G., "Boundary Search and Decomposition Method for MDO Problems with a Convex State Parameter Region," 4th Aerospace Sciences Meeting and Exhibit, Reno, NV, AIAA Paper 2005-0128, 2005.
- [11] Burden, R. L., and Faires, J. D., *Numerical Analysis*, 7th ed., Brooks/Cole, Pacific Grove, CA, 2000, Chaps. 7, 10.
- [12] Alexandrov, N. M., and Lewis, R. M., "Algorithmic Perspectives on Problem Formulations in MDO," 8th AIAA/USAF/NASA/ISSMO Symposium on Multidisciplinary Analysis and Optimization, Long Beach, CA, AIAA Paper 2000-4719, 2000.
- [13] Sobieszcanski-Sobieski, J., "Optimization by Decomposition: A Step from Hierarchic to Non-Hierarchic Systems," NASA CP-3031, Part 1, Sept. 1988.
- [14] Hajela, P., Bloebaum, C. L., and Sobieszcanski-Sobieski, J., "Application of Global Sensitivity Equations in Multidisciplinary Aircraft Synthesis," *AIAA Journal*, Vol. 27, No. 12, Dec. 1990, pp. 1002–1010.
- [15] Sobieszcanski-Sobieski, J., "Sensitivity of Complex, Internally Coupled Systems," *AIAA Journal*, Vol. 28, No. 1, Jan. 1990, pp. 153–160.
- [16] Renaud, J. E., and Gabriele, G. A., "Sequential Global Approximation in Non-Hierarchic System Decomposition and Optimization," *Advances in Design Automation*, Vol. 32-1, American Society of Mechanical Engineers, New York, 1991, pp. 191–200.
- [17] Renaud, J. E., and Gabriele, G. A., "Improved Coordination in Non-Hierarchic System Optimization," *AIAA Journal*, Vol. 31, No. 12, Dec. 1993, pp. 2367–2373.
- [18] Sobieszcanski-Sobieski, J., Agte, J. S., and Sandusky, R., Jr., "Bilevel Integrated System Synthesis," *AIAA Journal*, Vol. 38, No. 1, Jan. 2000, pp. 164–172.
- [19] Kodiyalam, S., and Sobieszcanski-Sobieski, J., "Bilevel Integrated System Synthesis with Response Surface," *AIAA Journal*, Vol. 38, No. 8, Aug. 2000, pp. 1479–1485.
- [20] Kroo, I., Altus, S., Braun, R., Gage, P., and Sobieski, I., "Multidisciplinary Optimization Methods for Aircraft Preliminary Design," 5th AIAA/USAF/NASA/ISSMO Symposium on Multidisciplinary Analysis and Optimization, Panama City Beach, FL," AIAA Paper 94-4325, Vol. 1, 1994, pp. 697–707.
- [21] Braun, R. D., and Kroo, I. M., "Development and Application of the Collaborative Optimization Architecture in a Multidisciplinary Design Environment," *Multidisciplinary Design Optimization: State of the Art*, edited by N. M. Alexandrov, and M. Y. Hussaini, Society for Industrial and Applied Mathematics, Philadelphia, 1997, pp. 98–116.
- [22] Braun, R., Gage, P., Kroo, I., and Sobieski, I., "Implementation and Performance Issues in Collaborative Optimization," 6th AIAA/NASA/ISSMO, Symposium on Multidisciplinary Analysis and Optimization, Bellevue, WA, AIAA Paper 96-4017, 1996.
- [23] Sobieski, I. P., and Kroo, I. M., "Collaborative Optimization Using Response Surface Method," *AIAA Journal*, Vol. 28, No. 10, Oct. 2000, pp. 1931–1938.
- [24] Alexandrov, N. M., and Lewis, R. M., "Analytical and Computational Aspects of Collaborative Optimization," NASA TM-2000-210104, 2000.
- [25] Alexandrov, N. M., and Lewis, R. M., "Comparative Properties of Collaborative Optimization and Other Approaches to MDO," NASA CR-1999-209354, 1999; also Inst. for Computer Applications in Science and Engineering, Rept. 99-24, 1999.
- [26] Wang, D., Wang, G. G., and Naterer, G. F., "Collaboration Pursuing Method for MDO Problems," First AIAA Multidisciplinary Design Optimization Specialist Conference, Austin, TX, AIAA Paper 2005-2204, 2005.
- [27] Wang, D., "Multidisciplinary Design Optimization with Collaboration Pursuing and Domain Decomposition: Application to Aircraft Design," Ph.D. Dissertation, Mechanical and Manufacturing Dept., Univ. of Manitoba, Winnipeg, Manitoba, Canada, May 2005.
- [28] Wang, D., "Study of Collaboration Model," Univ. of Manitoba, Technical Rept., Winnipeg, Manitoba, Canada, May 2005.
- [29] Haykin, S., *Neural Networks, A Comprehensive Foundation*, 2nd ed., Prentice-Hall, Upper Saddle River, NJ, 1999, Chap. 5.
- [30] Micchelli, C. A., "Interpolation of Scattered Data: Distance Matrices and Conditionally Positive Definite Functions," *Constructive Approximation*, Vol. 2, No. 1, Dec. 1986, pp. 11–22.
- [31] Wang, L., Shan, S., and Wang, G. G., "Mode-Pursuing Sampling Method for Global Optimization on Expensive Black-Box Functions," *Engineering Optimization*, Vol. 36, No. 4, Aug. 2004, pp. 419–438.
- [32] Shan, S., and Wang, G. G., "An Efficient Pareto Set Identification Approach for Multi-Objective Optimization on Black-box Functions," *Journal of Mechanical Design*, Vol. 127, No. 5, 2005, pp. 866–874.
- [33] Moré, J. J., and Sorensen, D. C., "Computing a Trust Region Step," *SIAM Journal on Scientific and Statistical Computing*, Vol. 4, No. 3, 1983, pp. 553–572.
- [34] Pérez, V. M., and Renaud, J. E., "Adaptive Experimental Design for Construction of Response Surface Approximations," 42nd AIAA/ASME/ASCE/AHS/ASC Structures, Structural Dynamics, and Materials Conference, Seattle, WA, AIAA Paper 2001-1622, 2001.
- [35] Tappeta, R., Nagendra, S., Renaud, J. E., and Badhrinath, K., "Concurrent Sub-Space Optimization (CSSO) MDO Algorithm in iSIGHT, CSSO in iSIGHT: Validation and Testing," General Electric Co., Corporate Research and Development Center, Schenectady, NY, Class 1 Rept. 97CRD186, Jan. 1998.
- [36] Kott, G., Gabriele, G. A., and Korngold, J., "Application of Multidisciplinary Design Optimization to the Power Stage Design of A Power Converter," *Advances in Design Automation*, Vol. 2, American Society of Mechanical Engineers, New York, 1993, pp. 359–366.
- [37] MATLAB, Software Package, Ver. 6.0, The MathWorks, Inc., Natick, MA, 2003.
- [38] Wang, D., Wang, G. G., and Naterer, G. F., "Advancement of a Collaboration Pursuing Method," 44rd AIAA Aerospace Sciences Meeting and Exhibit, Reno, NV, AIAA Paper 2006-0730, 2006.

A. Messac
Associate Editor